Title: Low Temperature Plasma-Catalytic NO_x Synthesis in a Packed DBD Reactor: Effect of Support Materials and Supported Active Metal Oxides

Author: B.S. Patil N. Cherkasov J. Lang A.O. Ibhadon V. Hessel Q. Wang

PII: S0926-3373(16)30328-9
DOI: http://dx.doi.org/doi:10.1016/j.apcatb.2016.04.055
Reference: APCATB 14740

To appear in: *Applied Catalysis B: Environmental*

Received date: 15-2-2016
Revised date: 20-4-2016
Accepted date: 27-4-2016

Please cite this article as: B.S.Patil, N.Cherkasov, J.Lang, A.O.Ibhadon, V.Hessel, Q.Wang, Low Temperature Plasma-Catalytic NOx Synthesis in a Packed DBD Reactor: Effect of Support Materials and Supported Active Metal Oxides, Applied Catalysis B, Environmental http://dx.doi.org/10.1016/j.apcatb.2016.04.055

Low Temperature Plasma-Catalytic NO_x Synthesis in a Packed DBD Reactor: Effect of Support Materials and Supported Active Metal Oxides

B. S. Patil[1], N. Cherkasov[2], J. Lang[3], A. O. Ibhadon[2], V. Hessel[1], Q. Wang[1#]

[1]Micro Flow Chemistry and Process Technology, Eindhoven University of Technology, P. O. Box 513, 5600 MB Eindhoven, Netherlands

[2]Catalysis and Reactor Engineering Research Group, Department of Chemistry and SOBBES, University of Hull, Cottingham Road, Hull, HU6 7RX, United Kingdom

[3]Innovation Management, Verfahrenstechnik & Engineering, Evonik Industries AG, Rodenbacher Chaussee 4, 63457 Hanau-Wolfgang, Germany

[#]corresponding author: Qi Wang, email: Q.Wang1@tue.nl, tel. +31(0)40 247 8290

Graphical Abstract:

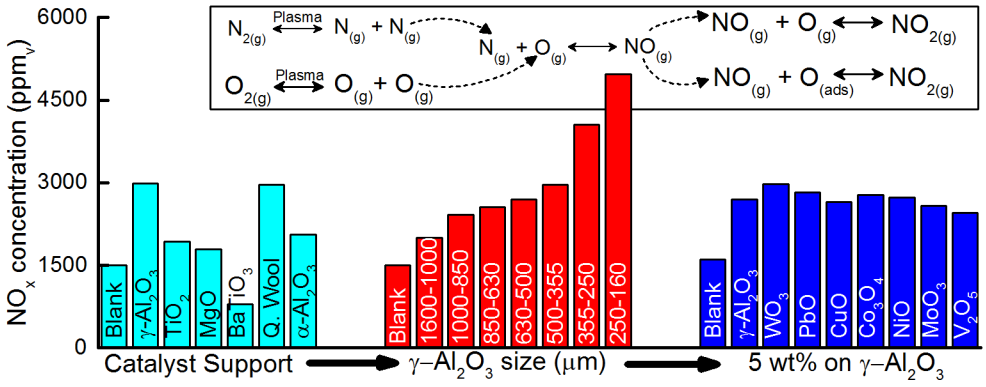

Highlights:

- Plasma-catalytic NO_x formation was studied at atmospheric P and low T using a range of materials
- Sharp edges and high surface area of plasma catalysts enhance NO_x formation
- Catalyst particles with 0.2 mm diameter produced 2.5 times higher NO_x than 1.3 mm
- Active metal oxides enhanced NO oxidation to NO_2

ABSTRACT

The direct synthesis of NO_x from N_2 and O_2 by non-thermal plasma at atmospheric pressure and low temperature is presented, which is considered to be an attractive option for replacement of the Haber-Bosch process. In this study, the direct synthesis of NO_x was studied by packing different catalyst support materials in a dielectric barrier discharge (DBD) reactor. The support materials and their particle sizes both had a significant effect on the concentration of NO_x. This is attributed to different surface areas, relative dielectric constants and particles shapes. The nitrogen could be fixed at substantially lowered temperatures by employing non-thermal plasma-catalytic DBD reactor, which can be used as an alternative technology for low temperature synthesis. The γ-Al_2O_3 with smallest particles size of 250-160 μm, gave the highest concentration of NO_x and the lowest specific energy consumption of all the tested materials and particle sizes. The NO_x concentration of 5700 ppm was reached at the highest residence time of 0.4 sec investigated and an N_2/O_2 feed ratio of 1 was found to be the most optimum for NO_x production. In order to intensify the NO_x production in plasma, a series of metal oxide catalysts supported on γ-Al_2O_3 were tested in a packed DBD reactor. A 5 % WO_3/ γ-Al_2O_3 catalyst increased the NO_x concentration further by about 10 % compared to γ-Al_2O_3, while oxidation catalysts such as Co_3O_4 and PbO provided a minor (~5 %) improvement. These data suggest that oxygen activation plays a minor role in plasma catalytic nitrogen fixation under the studied conditions with the main role ascribed to the generation of microdischarges on sharp edges of large-surface area plasma catalysts. However, when the loading of active metal oxides was increased to 10%, NO selectivity decreased, suggesting possibility of thermal oxidation of NO to NO_2 through reaction with surface oxygen species.

Keywords: plasma catalysis, nitric oxides, catalyst support, support particle size, supported active metal oxides.

1. Introduction

Nitrogen, being an important constituent of amino acids, is essential for life on earth [1–3]. However, this abundant element of atmosphere is hardly accessible to most living beings, because of the extremely stable N-N triple bond, which demands unusually high activation energy barrier. To become accessible, nitrogen must be chemically bonded to oxygen or hydrogen through the process of nitrogen fixation [1]. Nitrogen is artificially fixed with hydrogen through the Haber-Bosch process producing ammonia. This process sustains 40 % of today's population and its role will only grow along with the rapidly growing global population [1,4–7]. However, the Haber-Bosch process developed at the beginning of the 20th century is notoriously energy-inefficient. It consumes almost 2 % of world's total energy production and emits 300 million metric tons of CO_2 [8,9]. Modern technological and ecological standards require a considerable reduction in its environmental footprint and an increase in its energy efficiency. Nevertheless, the modern Haber-Bosch process has almost reached its theoretical limits on energy efficiency, so further improvements require a thorough search for a totally different approach [10].

Among several alternatives, electricity-driven plasma processes are considered to be very attractive candidates for the Haber-Bosch replacement. The idea arises from the thermodynamically non-equilibrium nature of non-thermal plasma (NTP), where electrons have a temperature of thousands of degrees, while the bulk gas is close to room temperature [11,12]. As a result, highly reactive species are formed enabling NTPs to conduct thermodynamically unfavorable reactions at low temperatures [11]. Unfortunately, the reactions taking place in NTP are difficult to control and the selectivity is rarely optimum towards the desired products. Hence, NTP is combined with heterogeneous catalysis through *Plasma Catalysis*, and it is a rapidly growing research area [13–17]. Plasma enables reactions at low temperatures and at faster rates, whereas catalysts increase reaction selectivity [14,15,18]. When plasma and catalysts are combined, they have very strong interactions and often yields a synergetic effect. Presence of catalyst is known to influence plasma discharge by enhancing the electric field, by changing the discharge type, and by facilitating micro-discharge formation in catalyst pores. Similarly catalyst's exposure to plasma changes its morphology, reduces metallic oxide to metallic catalyst [19,20]. Non-thermal plasma-catalyst systems have been effectively investigated for a range of processes such as CO_2 conversion to value added products [14,21], CH_4 reforming [22–24], volatile organic compound abatement [25–28], and automotive applications [18,29].

It is striking to note that nitrogen fixation via NTP, has a theoretical energy consumption 3 times lower than the Haber-Bosch process [10], offering a possibility of a fossil-free nitrogen fixation using renewable electricity with a fraction of the current energy costs [30,31]. Compared to the high-pressure Haber-

Bosch process, plasma nitrogen fixation offers an opportunity for atmospheric pressure and ambient temperature reactions with substantially improved plant safety, decreased operational and capital costs, although it will add new (electrical) equipment to the process such as transformer and electrical power supply system which are needed for plasma generation.

The plasma processes are more attractive on a smaller scale such as a container or modular plant [32]. The concept of de-centralized production of chemicals is gradually gaining an acceptance in chemical industry [33–35], and hence, opens new doors for containerized plasma nitrogen fixation process. This development would benefit remote and stranded areas in enabling them to produce their own fertilizer and fuels, using only renewable energy sources such as solar or wind [30,36–39].

Despite the important advantages, catalytic plasma nitrogen fixation is rather poorly studied [10,30,36]. Plasma catalytic NO_x synthesis was investigated by Cavadias and Amouroux in inductively coupled high frequency plasma reactor coated with catalysts such as MoO_3 and WO_3 [40]. The yield of NO_x was about 8 % without catalyst, but increased to 19 % by using the WO_3 catalyst. Mutel *et al.* [41] used the same metal oxides deposited on the plasma reactor wall. The energy consumption for catalytic nitrogen fixation process was found to be 0.93 MJ/mol of N, which provided a 78 % improvement in energy efficiency compared to thermal plasma process [41]. However, this energy consumption numbers are still far away from the energy consumption by Haber-Bosch process (i.e. 0.48 MJ/mol), which uses thermal catalysis. Belova *et al.* [42,43] investigated plasma catalytic nitric oxide synthesis in a glow discharge reactor and found the following order of catalyst effectiveness Pt>CuO>Cu>Fe>Ag [42,43]. Recently, Cu-ZSM-5 catalyst was investigated by Sun *et al.* [44] for NO_x formation in DBD reactor with a single stage configuration, where temperatures above 350°C was found favorable for NO_x formation [44]. Plasma-catalysis assisted ammonia synthesis in a DBD reactor is also reported in the literature as an alternative to thermal catalysis process, however the energy efficiency and yields are far from the current commercial process [30,45–47]. Nevertheless, to the best of our knowledge, no follow-up literature was published or commercial process developed, acknowledging and explaining the obvious synergetic effect of the catalyst in the results obtained. Similarly, various catalytic materials such as a range of metal oxides and metal-exchange zeolites were patented for plasma nitrogen fixation applications [48,49]. However, no independent studies of these catalysts have been published to assess their suitability for plasma NO_x synthesis and no systematic work exists covering the performance parameters of the plasma reactor.

The analysis of existing literature shows that very few catalysts have been systematically studied for plasma catalytic NO_x synthesis in NTP. Moreover, no study has been carried out to explain the reasons for the synergetic effect between plasma and catalyst. In particular, there are a number of overlapping reasons for the synergetic effect between the plasma and catalyst, e.g. influences caused by the different

support material, the different active catalyst and process parameters, etc. The decoding of such a complex topic needs a systematic approach in a simplified way. Till now, the information on the effect of catalyst support materials and reactor performance parameters on NO_x synthesis are scarce. Therefore, in this paper, we aim for a systematic study of plasma NO_x synthesis on supported oxide catalyst in a one-sided DBD reactor. Firstly, the effect of catalyst support, its dielectric properties, porosity, particle size and shape are investigated. Secondly, the main process parameters such as residence time and feed ratio are studied. Finally, a series of active metal oxides supported on the optimal support are tested.

2. Experimental section

2.1. 1-SDBD Plasma-Catalytic Reactor

Plasma NO_x synthesis was performed in a one-sided DBD plasma reactor at atmospheric pressure with a bed of catalytic material placed in the discharge zone. The schematic of the experimental set-up is shown in Fig. 1. Two different configurations of 1-SDBD reactor were used. Both reactor configurations consisted of an axial stainless steel (SS) inner high voltage electrode and a ground electrode made of SS mesh tightly wrapped around the quartz reactor body and a support/catalysts were embedded in the plasma zone. The discharge gap of 2 mm and the length of the discharge zone of 60 mm were identical for both reactor configurations. For the catalyst support experiments, the high voltage electrode was 20 mm o.d. and the quartz reactor body was 24 mm i.d. For the supported catalyst experiments, these dimensions were 6 and 10 mm, respectively. In the latter case, the small volume of the reactor allowed for tests with a small amount of the catalyst (about 2 g) compared to ~10-20 g used in the larger reactor. The reactors were placed in a tubular furnace to heat only the plasma discharge (catalyst) zone, while keeping the reactor ends outside of the furnace (shown in Figure SI-11 of supplementary information).

Both reactors were powered by a customized Xenionik EP 4000 alternating current power supply consisting of a signal generator (Siglent SDG 1025), a 4 kW audio amplifier (Behringer EP 4000) and a high voltage transformer (Xenionik). The applied voltage was measured using a high voltage probe (Tektronix P6015A) near the high voltage electrode. The capacitor (100nF) voltage was measured using 1:10 voltage probe on the grounded side as shown in Fig. 1. The power consumed by the DBD plasma reactor was calculated using the Lissajous method [50], based on the area of the plot between the applied and the capacitor voltages. All the electrical signals were recorded using a USB powered 4 channel PC Oscilloscope (PicoScope® 3000). The equations used to calculate the total power (P_{tot}), specific energy input (SEI), and the energy consumption per mole of NO_x (E_{NOx}) are shown in Eq. (1-3), respectively.

$$P_{tot} = f\ C_p \int_{onecycle} V(t)\, dV \qquad (1)$$

$$SEI = {}^{P_{tot}}\!/_{Q_{gas}} \quad (2)$$

$$E_{NOx} = {}^{P_{tot}}\!/_{(C_{NOx}\, Q_{gas})} \quad (3)$$

Where V is the applied voltage, C_p - capacitance of the capacitor, f - applied voltage frequency, Q_{gas} - volumetric gas flow rate, C_{NOx} - concentration of NO_x in gas.

Flow rates of N_2 and O_2 gases (Linde Gases, 99.9%) introduced into the reactor were controlled using mass flow controllers (Bronkhorst). The reaction products were analyzed online in the gas cell with CaF_2 windows (Specac) using a Fourier transform infrared spectrophotometer (Shimadzu IRTracer-100) at the resolution of 0.5 cm^{-1}. The concentrations of NO and NO_2 were determined by the adsorption bands at 1900 cm^{-1} and 1630 cm^{-1}, respectively, using a series of calibration gas mixtures. The concentration of NO_x was determined as a sum of NO and NO_2 concentrations. In all the experiments, full spectra were recorded and the main products were NO and NO_2. In a few experiments, N_2O was detected, but its concentration was negligible (N_2O intensity was more than 20 times lower than that of NO_2). Ozone was not detected, because it might have quickly oxidized NO to NO_2, even if formed. In all the cases, N_2 and O_2 conversion was below 0.5 %. Hence, NO selectivity reported was calculated using Eq. 4,

$$Selectivity\ NO = \ = C_{NO}/(C_{NO} + C_{NO2}) \quad (4)$$

The operation frequency and the pulse width were optimized in the range of 1–40 kHz and 15–30 μs, respectively, to achieve the highest NO_x concentration. For the bigger reactor, the frequency of 18 kHz and the pulse width of 20 μs was found to be the optimum. Whereas for the smaller reactor, the optimum frequency was 21 kHz and the pulse width 25 μs. The tested material was kept in-place by quartz wool (Carl Roth GmbH) positioned outside the catalyst bed.

Before every experiment, the reactor was heated to 150 ^oC with pre-heated nitrogen flow of 1 L/min to dry the tested support/catalysts. All the experiments were performed twice and all reported data were obtained as an average of at least 10 values obtained. The temperatures of the plasma region and the gas outlet were monitored continuously with thermocouples. For monitoring the plasma region temperature, the thermocouple was installed externally 1.5 cm away from the grounding electrode, the maximum temperature was found to be 200 ^oC. The outlet product stream temperature was always less than 26 ^oC. Heat transfer calculations based on heat fluxes in the reactor and introduced power showed that temperature inside the reactor was lower than 250^oC. Blank experiments with thermal (non-plasma) catalysis were performed up to the temperature of 400 ^oC and neither NO nor NO_2 were detected. Hence, all NO_x obtained was formed during plasma and plasma-catalytic processes.

2.2. Support and Catalyst Preparation

The support materials investigated in this work, γ-Al_2O_3, α-Al_2O_3, TiO_2, MgO, and $BaTiO_3$ were purchased (Mateck GmBh) in the form of ~3 mm pellets, crushed and sieved into a series of particle fractions for at least 24 h using a mechanical shaker until constant weight.

Supported catalysts were prepared using conventional wet impregnation techniques using pelletized γ-Al_2O_3 support. Active materials were selected to study the effect of oxygen binding energy as well as the performance of partial oxidation catalyst. About 50 g of the support was placed into a 1 L round-bottom flask, 500 mL of the precursor aqueous solution was added. Water was slowly evaporated by rotavapor for 5 h at 40 ^oC. The samples were placed in a tube furnace and dried at 110^oC for 4 h (heating rate 1 ^oC/min) and calcined for 2 h at 400 ^oC in air. The amount of the precursor was taken to obtain the active component (oxide) loading of 5 or 10 wt %. The following precursors were used: cobalt (II) nitrate (Alfa Aesar, >98 wt %) for Co_3O_4, oxalic acid dihydrate (Sigma-Aldrich, >99 wt %) and ammonium heptamolybdate (Fluka, >99 wt %) in 3:1 molar ratio for MoO_3, nickel (II) nitrate hydrate (Alfa Aesar, >98 wt %) for NiO, oxalic acid and ammonium metavanadate (Alfa Aesar, >99 wt %) in 3:1 molar ratio for V_2O_5, copper (II) nitrate (Alfa Aesar, >99 wt %) for CuO, ammonium tungsten oxide hydrate (Alfa Aesar, >99 wt %) for WO_3, lead (II) nitrate (Alfa Aesar, >99 wt %) for PbO.

2.3. Characterization of Support and Catalyst

Surface areas and pore distributions were measured by N_2 physiosorption using a TriStar 3000 micrometrics surface area and porosity analyser using standard multipoint Brunauer-Emmett-Teller (BET) analysis and Barrett Joyner Halenda (BJH) pore distribution methods. All specimens were dried at 150 ^oC for 1 h before the measurements in nitrogen flow. The results are presented in Table 1. All the materials except γ-Al_2O_3 and TiO_2 were non-porous (V_{pore}<0.5 μL/g). Average pore diameter for γ-Al_2O_3 was 15.5 nm and for TiO_2 – 16.6 nm. Nitrogen adsorption isotherm and a corresponding pore size distribution of γ-Al_2O_3 is presented in Fig SI-1, Supplementary Data.

Scanning electron microscopy (SEM) study was performed on the Zeiss EVO 60 instrument equipped with an energy-dispersive X-ray spectrometer Oxford instruments Inca System 350 under the pressure of 10^{-2} Pa and electron acceleration voltage of 20 kV. Powdered samples as well as fractured pellets were studied by applying them on conductive tape followed by carbon-coating before the SEM analysis.

Powder X-ray diffraction measurements of crushed samples were performed using an Empyrean powder X-ray diffractometer equipped with a monochromatic Kα-Cu X-ray source in the 2θ range of 10-80^o, step length 0.026^o, step time 147 s. The X-ray diffraction measurements are presented in SI-2. The

characterisation was performed before and after the plasma catalytic tests and no differences in either textural and chemical properties of the catalysts were observed.

3. Results and discussion

3.1. Effect of support material

3.1.1. Effect on NO_x production

To understand the effect of the different support materials on NO_x production, experiments were conducted with 500-630 µm particles (except quartz wool) at varying specific energy input and flow rate of 1 L/min with N_2:O_2 volume ratio of 1. Support materials studied were γ-Al_2O_3, α-Al_2O_3, MgO, TiO_2, $BaTiO_3$ and quartz wool. A blank experiment was also conducted without packing to compare with the packed bed experiments.

In Fig. 2a, the concentration of NO_x is plotted against the SEI for different supports. The input power was in the same range for all the tested catalyst supports. The effect of the packed catalyst support on NO_x production is clearly visible, the NO_x concentration increases proportionally with SEI for all support materials. The SEI for quartz wool, MgO, γ-Al_2O_3, α-Al_2O_3 and the blank experiment fall in the same range of 2000 to 4000 J/L with varying concentration of the NO_x from 700 to 3000 ppm. Comparing these catalyst supports shows that the blank experiment without packing any catalyst support always has the lowest NO_x concentration at the same SEI. Whereas, the γ-Al_2O_3 gave the highest NO_x concentration. At the SEI of 4000 J/L, γ-Al_2O_3 gives a 100% increase in the NO_x concentration compared to the blank experiment. Quartz wool was also found to be an efficient catalyst support for NO_x generation, similar to γ-Al_2O_3.

The results obtained for the higher relative dielectric constant supports such as TiO_2 and $BaTiO_3$ are located in a lower range of SEI (< 2500 J/L). The NO_x concentrations for these two packed materials are similar at SEI higher than 1250 J/L. However, for these materials at comparable SEI, NO_x concentrations are substantially lower, indicating the fact that the plasma discharge might be less intense and was in the form of glow discharge.

Another important criteria is the selectivity of support materials to produce either NO or NO_2. In Fig. 2b, the selectivity towards NO is plotted against the SEI. The selectivity towards NO for all the materials studied lies around 50 % in the SEI range from 1500 to 3800 J/L, while it changes non-linearly at a lower SEI reaching more than 90 % for $BaTiO_3$ and TiO_2 at the lower SEI studied. On the contrary, at a higher energy input (> 3800 J/L), the NO selectivity slowly decreased. These trends suggest that nitrogen

fixation in NTP initially occurs in the form of NO. When the energy input increases, chances of NO oxidation increase, resulting in the increasing formation of NO_2. The NO selectivity for γ-Al_2O_3 is lower than quartz wool, even though both of them produced equally high concentration of NO_x. This difference in NO selectivity for γ-Al_2O_3 and quartz wool suggests the possibility of reaction of NO species with surface adsorbed oxygen species on γ-Al_2O_3 to yield higher amount of NO_2. Based on the results from this study, one can choose the SEI range and the catalyst support to obtain the desired product.

3.1.2. Reasons of varied effect on NO_x production with different support material

Discharge Behavior

The electrical signals for various support materials can provide important information on discharge behavior of the studied systems. Even though the signal generator supplies energy in the form of pulses with a frequency of 18 kHz and a pulse width of 20 μs, the voltage and current signal measured on the DBD reactor was quasi-sinusoidal for all the packing materials investigated, as shown in Fig. 3.

As can be seen from Fig. 3, the spikes on the capacitor voltage /current were different for different materials and resulted in different discharge behaviors as shown in the characteristic photographs presented in SI-7 of the Supplementary Material. These spikes are characteristic for the formation of the microdischarges (filamentary discharges) in DBD reactor [27,51]. As reported for the standard one-sided DBD without packing, the microdischarge crosses the complete discharge gap, starting from the inner electrode to the surface of the dielectric. When the discharge gap was packed with support material, the available space for the filamentary microdischarge formation became limited. Thus, only weak microdischarges were generated in-homogeneously in the void space between pellets and between pellets and the dielectric wall as well as pellets and the high voltage electrode. Along with filamentary discharges, surface discharges were formed and propagated over the support material surface [52,53]. Therefore, the filamentary discharge formed in the DBD reactor without packing transits into the combination of localized weak filamentary discharges and surface discharges in case of the packed bed DBD reactor [52].

When the discharge gap is packed with catalyst support, the microdischarges cannot travel on the same tracks any more. It can be noticed from V-I curve of γ-Al_2O_3 packed DBD and without packed DBD that they are quite similar. Thus, it can be concluded that there were microdischarges generated between the particles surfaces or between the particles and electrode/dielectric in case of γ-Al_2O_3 packed DBD. However, for $BaTiO_3$, no obvious spikes were identified demonstrating that no microdischarges had been formed. Minor surface discharges might have occurred at the catalyst surface resulting in low NO_x formation. For MgO and TiO_2, the spikes were moderate but weaker than the blank experiment, which demonstrated the formation of weak microdischarges. It is also worth noting that the quartz wool had the highest amplitude for current and capacitor voltage spikes, which mean that the microdischarges

generated in case of quartz wool were stronger than the other catalyst supports. Such a difference between discharge behaviors of quartz wool and γ-Al_2O_3 can also explain the difference in NO selectivity (Fig. 2b). More intensive plasma generation in case of quartz may have resulted in larger amount of high-energy species to form NO.

As a result, various materials provide substantially different discharge behavior, either improving or suppressing the formation of microdischarges. From the comparison of the V-I signals and NO_x concentration data, it is clear that the formation of microdischarges is essential for the nitrogen fixation. The possible reasons for the different V-I behavior of the materials studied are the differences in relative dielectric constant, surface area, or particle shape. The detailed analysis of these factors is provided below. However, it should be mentioned that other parameters such as surface electrical conductivity and presence of nanofeatures generating high electric field may also contribute. Therefore, further controlled experiments are required to elucidate these parameters.

Surface area

As shown in Fig. 2a, the γ-Al_2O_3 catalyst support, with the highest surface area, gave the highest NO_x concentration (

). A more direct comparison between γ-Al_2O_3 and α-Al_2O_3, which have a similar chemical functionality and close relative dielectric constants, shows that the surface area is crucial for plasma nitrogen fixation.

Surface area is known to be essential for conventional (thermal) heterogeneous catalysis for extensive reasons. A high surface area in a catalyst provides more active sites; or alternatively, a catalyst support with a higher area generally holds smaller metal nanoparticles with larger active (metal) area. In the case of plasma catalysis, the reaction is activated by the microdischarges between the particles or between particles and electrode/dielectric. The discharge area without any packing material is only the area of the reactor walls. In the presence of the packing particles, the discharges happen mainly on the surface of the particles as observed in other studies [54]. Hence, the higher surface area is considered to lead to higher frequency of discharges resulting in higher NO_x concentration. Similarly, an empty DBD reactor has a negligible geometric area of its walls and is the reason for the lowest NO_x concentration observed (Fig. 2a).

Relative dielectric constant

As described in the section 3.1.1, at the same input power, the NO_x concentration obtained with TiO_2 and $BaTiO_3$ catalyst supports was much lower compared even to the blank experiment. The relative dielectric constants of TiO_2 and $BaTiO_3$ are much higher than that of other materials (

), which suggests an important role of the relative dielectric constant on NO_x plasma synthesis. For a comparison, the blank experiment can be considered as an experiment with a relative dielectric constant of 1 for the *packing material*, which is the mixture of N_2 and O_2. All the other materials have a relative

dielectric constant lower than 10, while TiO_2 has 85 and $BaTiO_3$ has in the range of 600-4500 depending on temperature [55].

The relative dielectric constant is an indication about how easily a material can be polarized when an electric field is applied. A higher relative dielectric constant means a material can polarize more easily when an electric field is applied and a polarized material creates an internal electric field which opposes the overall electric field. This gives a lower overall electric field and results in decreased energy of electrons. In other words, the voltage on the packing material (U_p) depends on the relative dielectric constants of the gas phase (ε_g) and packing material (ε_p) as well as mean gap thicknesses in the gas (d_g) and the solid respectively (d_p) as shown in Eq. 5 [54].

$$U_p = U_g \frac{\varepsilon_g}{\varepsilon_p} \frac{d_p}{d_g} \qquad (5)$$

Thus, with a higher relative dielectric constant, a lower voltage will be added to the packing material because the sum of U_p and U_g is the total voltage applied to the packed DBD reactor. In case of $BaTiO_3$, which has a very high relative dielectric constant, plasma ignition is very easy. As a result of lower voltage on the packaging material, electrons have lower acceleration and carry smaller energy. Smaller electron energy leads not only to a decrease in the energy of the reactive species, but also to decreased gas ionization as well. The latter happens because in a higher electric field, shorter distance is required for electrons to reach the ionization energy resulting in larger number of ionizations inside the fixed discharge gap. In our case, only very low plasma current could be observed when $BaTiO_3$ was used as support. Also, $BaTiO_3$ does not show the spikes in current or capacitor voltage signals, indicating the presence of glow (uniform discharge) instead of filamentary discharges. As a result, it was difficult to increase the SEI to $BaTiO_3$ packed DBD, even though the input energy was of the same magnitude as other supports. Thus, the results from $BaTiO_3$ are located in the lowest range in Figure 2a. When alumina, with a lower relative dielectric constant, was used as support for the reaction, intense plasma was visible. This also resulted in a higher concentration of NO_x (Fig. 2a).

Shape of the catalyst support

The surface area and the relative dielectric constant are not the only factors that affect NO_x formation because the quartz wool has shown very high NO_x concentration as γ-Al_2O_3. A possible explanation for this effect is the increase in electric field in places with highest curvature. Quartz wool has a fine fibrous structure with the rigid sharp edges which induces very high electric fields as reflected by the sharpest V-I spikes (Fig. 3e). Chen *et al.* [56] proved that the sharp edges of packing material led to higher local electric fields and highly energetic electrons [21]. Thus, the superior performance of quartz wool for NO_x production can be explained by fibrous sharp edge morphology.

Similarly, γ-Al_2O_3 also showed considerable number of high intensity peaks for current and voltage, which could be the result of the sharp edges on the particles as can be seen from the SEM pictures in (Figure SI-3). Analogous sharp edges can also be seen in case of $BaTiO_3$. For $BaTiO_3$, the effect of electric field enhancement by sharp edges could have been nullified by its comparatively high relative dielectric constant. Similarly, the shape considerations also worked for other materials. For example, the SEM shows that MgO and TiO_2 have much smoother edges in agreement with lower microdischarges and NO_x formation.

3.2. Effect of particle size

3.2.1. Effect on NO_x production

Results from this work show that particle shape has substantial effect on NO_x formation and γ-Al_2O_3 was found to be the most efficient catalyst support. As a result of this, the effect of γ-Al_2O_3 particle size on NO_x formation was studied further.

The concentration of NO_x increases proportionally with SEI for all particle sizes investigated as shown in Fig. 4a. There is a marked effect of particle size on the NO_x concentration. The smaller support particles gave higher concentration of NO_x as compared to the corresponding larger support particle. The highest NO_x concentration of 5000 ppm was achieved with smallest support particle (250-160 μm) tested. The reasons could be the changes in discharge behavior and void fraction which are discussed in the next section.

For all particle sizes, the NO selectivity decreased with the increasing SEI, as shown in Fig. 4b. The chances of NO oxidation increased with the corresponding increase in energy input, yielding higher amounts of NO_2. Although not linearly, but generally smaller particles favored NO_2 formation than NO formation. This is because the smaller particles exhibit higher discharge and surface area, which increases the electron energy as well as influences the residence time. These two factors contribute to the oxidation of NO to NO_2 during the course of the reaction. A previous study showed that the SEI and residence time are the two factors that lead to further oxidation of NO to NO_2 [57]. Here, the residence time is influenced by the void fraction which will be discussed below.

3.2.2. Reasons of varied effect on NO_x production with different particle sizes

Discharge behavior

First of all, the change of discharge behavior is the most straightforward explanation of particle size effect as can be seen from the V-I curves (Fig. 5). Comparing the current and voltage curves for various particle sizes, it can be noted that the particle size has a considerable effect on the intensity of spikes. For the smaller particles sizes, a higher amplitude of current fluctuations was observed demonstrating higher

intensity of microdischarges formed. As discussed in section 3.1.2, these high intensity spikes are the reason for the higher amount of NO_x produced. The smaller particles with sizes of 355-250 and 250-160 μm, generated a higher amount of NO_x likely due to the high intensity localized electric field generated at particle-particle, particle-electrode and particle-dielectric contact points. The decrease in the particle size also increases the exposed surface area of particle to the plasma discharge. These combinations of effects are responsible for higher amount of NO_x produced in smaller size particles.

Void fraction

Except for the discharge behavior, the void fraction was also changed. For the same reactor volume, the void fraction decreases with the decrease in particle size. This decrease in void fraction results in the higher number of contact points between support particles and between particle and electrode/dielectric, the points where electric field is stronger than the mean value in the reactor [22]. Hence, the discharge area must have been much higher and intense in case of DBD reactor packed with smaller particles than with the larger particle sizes. As a result, NO_x formation increased with the smaller particles, which is in good agreement with the results obtained for CO_2 conversion [21,22,54].

3.3. Effect of residence time

The mean residence time will affect the extent of the reaction in conventional thermal catalysis. Thus, the performance of DBD reactor with varying residence time was investigated with particles of γ-Al_2O_3 (500-355 μm) up to an acceptable pressure drop. Therefore, four residence times were investigated with a feed ratio (N_2/O_2) of 1 (Fig. 6). The residence time of 0.1 s, 0.13 s, 0.2 s and 0.4 s were achieved by changing the gas feed flowrate to 2, 1.5, 1, to 0.5 L/min, respectively.

Fig. 6a shows the effect of residence time and SEI on NO_x concentration. Concentration of NO_x increases proportionally to SEI for all residence times investigated. The highest concentration of 5670 ppm was achieved with SEI of 8980 J/L for residence time of 0.4 s.

Longer residence times results in a higher concentration of NO_x because of longer reaction times and the higher SEI per unit volume of the feed gases. Increase in residence time helps in the ionization and reaction of the maximum number of reactant species. Supplying a higher SEI per unit volume of reactants gives high mean energy to electrons to react and produces the reaction species, which lead to reaction to produce nitric oxide and NO_2.

Fig. 6b shows the selectivity to produce NO over NO_2. For the highest residence time, 0.4 s, the selectivity for NO decreases with the increased SEI, therefore NO_2 formation is favored over NO formation. At short residence time, i.e. 0.1 s, selectivity for NO formation increases. Thus, the NO_2 formation is favored over NO formation at lower residence time. With a long residence time inside the

discharge zone, NO is further oxidized to NO_2. Whereas with a short residence time, it is not sufficient for oxidation of NO to NO_2, therefore NO leaves in higher amount as final product.

3.4. Effect of Feed Ratio

The effect of feed ratio on NO_x synthesis was investigated by varying the feed ratio of N_2 to O_2 from 0 to 4. The effect of feed ratio on the concentration of NO_x and the selectivity of NO is shown in Fig. 7. A feed ratio of 1 to 1.5 was found to be optimum to produce higher amount of NO_x, similar to our previously published study on gliding arc reactor [57]. At a feed ratio of 1, reactive species of nitrogen and oxygen have equal probability to combine with adjacent oxygen and nitrogen species, respectively. The combination reaction gives NO first and then further oxidation yields NO_2.

As the ratio of N_2 to O_2 increases, NO is produced in higher amount than NO_2. For a ratio of 4, the selectivity of NO is 56 % and at the feed ratio of 0.25 the selectivity of NO is 35%. At a lower feed ratio meaning a higher feed rate of oxygen, the formation of NO_2 is favored more as the NO produced is readily further oxidized to NO_2 because of the higher proportion of O_2 in the feed.

3.5. Active Metal Oxides Supported Catalysts

In order to study the effect of catalyst in plasma nitrogen fixation, the best performing γ-Al_2O_3 support was selected and various metal oxides were deposited on it. Supported rather than single-phase catalysts were used, so the overall physical properties of the particles such as relative dielectric constant and shape were constant, apart from catalyst surface chemical properties which are determined by the supported active oxide. This combination provided a direct comparison of the plasma catalytic properties of the active metal oxide, rather than a combination of physical and chemical properties as has been previously performed.

The conventional catalysts for complete oxidation of hydrocarbons were selected for the study, because their main role in the thermal activation of oxygen species is thoroughly studied [58,59]. It is expected that in the plasma-catalytic nitrogen fixation, nitrogen species will be activated by the high-energy plasma species, then these species should react with the oxygen species either thermally activated by the catalysts or by plasma.

To study these hypotheses, a wide range of oxides with various degrees of oxygen activation abilities were supported. For example, alumina is almost inactive in oxygen activation, while PbO, CuO and Co_3O_4 provide quick oxidation of hydrocarbons with the activity inferior only to noble metals (Fig. SI-5 in the Supplementary Data) [58]. Noble metals were not considered in the current work, because highly conductive metallic particles have different electronic properties. In such a case, it would be impossible to attribute any observed differences in activity to the factor of chemical properties. Other oxides such as

NiO, MoO_3, V_2O_5 and WO_3 are expected to be of intermediate activity between Al_2O_3 and Co_3O_4, if oxygen activation step is crucial for nitrogen fixation.

These catalysts were characterized by nitrogen physisorption, powder X-ray diffraction and SEM. These results are given in Fig. SI-1, SI-2, SI-3 and SI-4 respectively in the Supplementary Data. They showed that the introduction of the active oxide on alumina did not affect its overall physical properties. Elemental mapping confirmed a uniform distribution of the oxides over the support.

3.5.1. Influence of Active Metal Oxides

Packing catalyst support or supported metal oxides in DBD clearly shows a considerable improvement in the amount of NO_x produced compared to the blank experiment conducted as shown in Fig. 8a. Also the SEI for all the performed experiments was the same, demonstrating that the assumption of supported metal oxides did not change the physical properties of the catalyst support is valid. The comparison of γ-Al_2O_3 with the supported catalysts does not show a large increase in NO_x concentration. However, the trends are in excellent agreement with the results of Gicquiel et al. [60], who showed that WO_3 provided the highest nitrogen fixation activity in plasma followed by MoO_3 and empty microwave discharge reactor.

The catalysts also affected the selectivity towards NO (Fig. 8b). For the blank experiment, the NO selectivity was the highest suggesting that the primary product of plasma nitrogen fixation, NO, had lower chances of further oxidation to form NO_2. For the plasma-catalytic nitrogen fixation, however, the results were unexpected. In particular, the most active 5% WO_3/Al_2O_3 catalyst showed the lowest activity suggesting that it increased either NO oxidation or provided an alternative direct route towards NO_2 formation. Surprisingly, the other two active catalysts 5% Co_3O_4/Al_2O_3 and 5% PbO/Al_2O_3 which showed similar NO_x concentrations demonstrated the different NO selectivities, 48 and 56 % respectively. Conversely, it was expected to obtain very similar results due to very similar oxygen activation properties of these two catalysts. Such a difference indicates that there exists a separate channel for NO_2 formation on certain catalysts. However, the mechanistic studies do not support the possibility of NO_2 formation as a product of plasma oxidation of N_2 [61,62]. As a result, the effect of the catalyst on NO selectivity could be explained in terms of localized discharge formation, i.e. enhancement of plasma formation in the catalyst vicinity allowing for higher plasma density, resulting in higher chances of secondary oxidation of NO either with plasma-activated oxygen species or with surface adsorbed oxygen species. The catalyst-dependent plasma formation near the surface was reported by Durme et al. [27].

Further comparison of the catalytic results has been performed following the known trends in complete catalytic oxidation of hydrocarbons, i.e. studying the effect of catalyst activity depending on oxygen "binding" energy [58]. Interestingly, there is only a minor correlation between the nitrogen fixation

activity in plasma and the activity in oxygen activation (Fig. 9). For example, PbO and Co_3O_4, which are the most active in oxygen activation, demonstrated only slightly higher NO_x concentration compared to γ-Al_2O_3. Also, the WO_3 catalyst showed NO_x concentration noticeably higher than expected based on its oxygen activation activity. These observations suggest that oxygen activation on the catalysts plays a role in plasma-catalytic nitrogen fixation. However, this role is much less important compared to thermal oxidation reaction probably because oxygen activation under the studied conditions takes place mostly in plasma as shown by the results obtained with all the supported catalysts which were closely similar. This means that the main role of plasma catalyst in nitrogen fixation is in the facilitation of microdischarge formation rather than the chemical interaction with the plasma-activated species.

Complete hydrocarbon oxidation usually takes place at elevated temperatures of 300-500 ^oC, but the studied reactions were performed at a reactor temperature of about 250 ^oC. As a result, it may result in insufficient oxygen activation on the catalyst surface and this may affect the conclusions drawn regarding the catalytic activity. This possibility and the influence of temperature between 200 and 400 ^oC for a selected NiO/Al_2O_3 catalyst has been studied and reported in supplementary information section SI-5. The results presented in Fig. SI-8 of the Supplementary information show that NO_x concentration slightly decreases at a higher temperature, which confirms that oxygen activation in plasma nitrogen fixation does not play an important role.

Influence of Active Metal Oxide Loading

To study the effect of the supported oxide on plasma nitrogen fixation, several selected catalysts with higher active metal contents were prepared. Fig. 10a shows that the NO_x concentrations for the 5 and 10 % active metal oxide loaded catalysts in plasma are very close, which supports the conclusion that active metal oxides play a minor role in plasma nitrogen fixation. Furthermore, the catalyst that contain 10 % of the active oxides is shifted to a lower SEI compared to that containing 5%, which indicates that for these catalysts not only surface chemical properties, but bulk physical properties discussed in 3.1 (e.g., relative dielectric constant), were substantially affected. Interestingly, the MoO_3 catalyst which was reported by several authors to be efficient in plasma nitrogen fixation showed rather marginal improvement compared to γ-Al_2O_3 [41,60].

However, the difference in catalyst performance was most clear while considering NO selectivity. Because, a well-known active oxidation catalyst, 10% Co_3O_4/Al_2O_3, provided enough active species for oxidation of NO into NO_2 (Fig. 10b). Even though, different loadings of metal oxides catalyst found not to change the concentration of NO_x much, the selectivity to NO_2 increased significantly for 10% loaded metal oxide catalysts, especially for Co3O4 as can be seen from Fig. 10b. It strongly suggests that the

activation of N_2 and O_2 mainly takes place in the plasma phase and the catalyst do play an important role in oxidation of NO to NO_2 through reaction with surface adsorbed O species.

4. Conclusions

A systematic study of the plasma catalytic nitrogen oxidation has been performed in a one-sided DBD reactor. A range of catalyst supports, α-Al_2O_3, γ-Al_2O_3, TiO_2, MgO, $BaTiO_3$ and quartz wool were studied, which showed completely different behavior. Quartz wool and γ-Al_2O_3 showed almost twofold increase in NO_x concentration compared to the blank experiment, while $BaTiO_3$ provided much lower concentration due to the formation of glowing discharge compared to numerous filamentous microdischarges that were obtained using other supports. Electrical characteristics of the microdischarges were studied and showed a direct correlation between the formation of microdischarges and NO_x formation. Hence, maximizing the formation of microdischarges seems to be an appropriate means of increasing nitrogen fixation in plasma.

The comparison of the physical properties of the investigated catalyst supports indicated that 3 characteristics contribute in facilitating microdischarges formation. Firstly, high surface area provides large area for the generation of the microdischarges because γ-Al_2O_3 (~100 m^2/g) showed about 30 % higher NO_x concentration compared to α-Al_2O_3 (<1 m^2/g). Secondly, moderate relative dielectric constant (<10), provides high voltage in the packing material and results in high NO_x concentration. In case of higher relative dielectric constants, the glowing discharge was observed for $BaTiO_3$, producing lower NO_x concentration. Thirdly, the presence of sharp edges where the electric field is high was an important factor. Rigid fibrous quartz wool provided enough sharp edges, where the electric field is stronger to generate high intensity microdischarges, which gave higher NO_x concentration similar to γ-Al_2O_3. Similarly, smaller particles provided smaller radii curvature, which increased NO_x formation by almost twofold when comparing γ-Al_2O_3 particles of 0.2 and 1.3 mm average diameter. However, at this stage it is impossible to rule out contribution of other effects such as surface electrical conductivity and presence of nanofeatures on the catalyst surface.

Results of gas residence time study in a plasma reactor packed with γ-Al_2O_3 showed that a higher gas flow rate increases energy efficiency by about 50 %, but decreases total NO_x concentration considerably in the gas. The gas ratio, N_2/O_2, of 1, was found to be optimum, with the other ratio in the range of 0.2–4 providing about 17 % decreased NO_x formation due to the preferential formation of the primary NO products from such a gas mixture.

The most important factors that increase the nitrogen fixation efficiency by almost 60 % compared to the blank experiment are catalyst's geometrical factors such as particle sizes and shapes. Hence, the main

role of the plasma catalyst seems to be the facilitation of the formation of microdischarges in plasma via large surface area and a large amount of sharp edges. Therefore, the catalyst supports which have high surface area in combination with sharp edges, such as 3D printed, could yield higher concentrations in plasma catalytic nitrogen fixation.

A range of metal oxides were supported on γ-Al_2O_3, which provided comparable physical properties of the catalysts and allowed for direct comparison of the effect of surface chemistry on the plasma nitrogen fixation. The supported catalysts showed rather marginal (at most 10 %) increase compared to the catalyst support used (γ-Al_2O_3). Interestingly, WO_3 was found to be the most active, while well-known oxygen activation catalyst such as PbO or Co_3O_4 showed much lower improvement of below 5 %. These data show that oxygen activation on complete combustion catalysts plays a role. It is likely that the vibrationally excited nitrogen species, which are known to be formed in plasma [60,61], have a higher probability of reaction with the mobile oxygen species on the catalyst surface. The marginal increase in selectivity shows that the non-catalytic route via direct gas-phase interaction of excited N_2 with O_2 species prevails. When the loading of active metal oxide was increased from 5% to 10%, the difference in catalysts activity was the most evident in case of 10% Co_3O_4/Al_2O_3, a well-known oxidation catalyst, which likely provided a large amount of activated oxygen to oxidize plasma-formed NO into NO_2.

Based on the results of the study, it is clear that further efforts are required to make plasma nitrogen fixation commercially feasible. Firstly, NO_x yield should reach an order of at least 1-2 vol. % for ease of separation. Secondly, the energy efficiency should be increased to a level comparable to that of the Haber-Bosch process. Even having the same energy efficiency, plasma nitrogen fixation could be a compelling business case provided by off-the-grid economy opportunities. For example, synthesis of nitrogen fertilizers in container-scale miniplants can be performed using local renewable energy resources such as wind and solar. At an industrial scale, plasma synthesis is promising by significant simplification of the plant equipment required.

Acknowledgement

This research is funded by the EU project MAPSYN: Microwave, Acoustic and Plasma SYNtheses, under the grant agreement no. CP-IP 309376 of the European Community's Seventh Framework Program.

Appendix A. Supplementary Data

Supplementary Data associated with this paper can be found in the online version of the paper and contains the following information: Nitrogen adsorption isotherm of pristine γ-alumina support, Powder X-ray diffraction patterns of the catalysts synthesised, SEM Images of catalyst supports and the supported active metal oxides, Volcano plot of catalytic activity for propylene oxidation on oxide catalysts, Temperature of catalyst bed and its effect on the NO_x concentration and NO selectivity, Energy Efficiency for Plasma NO_x Synthesis

References

[1] J.N. Galloway, E.B. Cowling, Reactive nitrogen and the world: 200 years of change., Ambio. 31 (2002) 64–71. doi:10.2307/4315217.

[2] V. Smil, Global Population and the Nitrogen Cycle, Sci. Am. 76 (1997).

[3] D.E. Canfield, A.N. Glazer, P.G. Falkowski, The evolution and future of Earth's nitrogen cycle., Science. 330 (2010) 192–6. doi:10.1126/science.1186120.

[4] E. Cowling, J. Galloway, C. Furiness, M. Barber, T. Bresser, K. Cassman, et al., Optimizing nitrogen management in food and energy production and environmental protection: summary statement from the Second International Nitrogen Conference., Sci. World J. 1 (2001) 1–9. doi:10.1100/tsw.2001.481.

[5] V. Smil, Enriching the Earth: Fritz Haber, Carl Bosch, and the Transformation of World Food Production, MIT Press, 2004.

[6] M. Appl, Ammonia, 2. Production Processes, Ullmann's Encycl. Ind. Chem. (2012) 139–225. doi:10.1002/14356007.o02.

[7] M. Appl, The Haber-Bosch Heritage: The Ammonia Production Technology, in: 50th Anniv. IFA Tech. Conf., 1997: p. 25.

[8] R.R. Schrock, Reduction of dinitrogen., Proc. Natl. Acad. Sci. U. S. A. 103 (2006) 17087. doi:10.1073/pnas.0603633103.

[9] J.W. Erisman, M.A. Sutton, J. Galloway, Z. Klimont, W. Winiwarter, How a century of ammonia synthesis changed the world, Nat. Geosci. 1 (2008) 636–9.

[10] N. Cherkasov, A.O. Ibhadon, P. Fitzpatrick, A review of the existing and alternative methods for greener nitrogen fixation, Chem. Eng. Process. Process Intensif. 90 (2015) 24–33. doi:10.1016/j.cep.2015.02.004.

[11] A. Fridman, Plasma Chemistry, Cambridge University Press, New York, 2008.

[12] M.A. Lieberman, A.J. Lichtenberg, Principles of Plasma Discharges and Materials Processing, Wiley, 2005.

[13] C.E. Stere, W. Adress, R. Burch, S. Chansai, a. Goguet, W.G. Graham, et al., Probing a Non-Thermal Plasma Activated Heterogeneously Catalyzed Reaction Using in Situ DRIFTS-MS, ACS Catal. 5 (2015) 956–964. doi:10.1021/cs5019265.

[14] A. Gómez-Ramírez, V.J. Rico, J. Cotrino, A.R. González-Elipe, R.M. Lambert, Low temperature production of formaldehyde from carbon dioxide and ethane by plasma-Assisted catalysis in a

ferroelectrically moderated dielectric barrier discharge reactor, ACS Catal. 4 (2014) 402–408. doi:10.1021/cs4008528.

[15] L. Wang, Y. Yi, Y. Zhao, R. Zhang, J. Zhang, H. Guo, NH $_3$ Decomposition for H $_2$ Generation: Effects of Cheap Metals and Supports on Plasma–Catalyst Synergy, ACS Catal. (2015) 4167–4174. doi:10.1021/acscatal.5b00728.

[16] J.C. Whitehead, Plasma catalysis: A solution for environmental problems, Pure Appl. Chem. 82 (2010) 1329–1336. doi:10.1351/PAC-CON-10-02-39.

[17] Y.-R. Zhang, K. Van Laer, E.C. Neyts, A. Bogaerts, Can plasma be formed in catalyst pores? A modeling investigation, Appl. Catal. B Environ. 185 (2016) 56–67. doi:10.1016/j.apcatb.2015.12.009.

[18] C.E. Stere, W. Adress, R. Burch, S. Chansai, A. Goguet, W.G. Graham, et al., Ambient Temperature Hydrocarbon Selective Catalytic Reduction of NOx Using Atmospheric Pressure Nonthermal Plasma Activation of a Ag/Al2O3 Catalyst, ACS Catal. 4 (2014) 666–673. doi:10.1021/cs4009286.

[19] E.C. Neyts, a Bogaerts, Understanding plasma catalysis through modelling and simulation—a review, J. Phys. D. Appl. Phys. 47 (2014) 224010. doi:10.1088/0022-3727/47/22/224010.

[20] E.C. Neyts, K. (Ken) Ostrikov, M.K. Sunkara, A. Bogaerts, Plasma Catalysis: Synergistic Effects at the Nanoscale, Chem. Rev. 115 (2015) 13408–13446. doi:10.1021/acs.chemrev.5b00362.

[21] X. Duan, Z. Hu, Y. Li, B. Wang, Effect of Dielectric Packing Materials on the Decomposition of Carbon Dioxide Using DBD Microplasma Reactor, AIChE J. (2014). doi:10.1002/aic.

[22] H.J. Gallon, X. Tu, J.C. Whitehead, Effects of Reactor Packing Materials on H2 Production by CO2 Reforming of CH4 in a Dielectric Barrier Discharge, Plasma Process. Polym. 9 (2012) 90–97. doi:10.1002/ppap.201100130.

[23] Q. Wang, B.-H. Yan, Y. Jin, Y. Cheng, Investigation of Dry Reforming of Methane in a Dielectric Barrier Discharge Reactor, Plasma Chem. Plasma Process. 29 (2009) 217–228. doi:10.1007/s11090-009-9173-3.

[24] X. Tu, H.J. Gallon, M. V Twigg, P. a Gorry, J.C. Whitehead, Dry reforming of methane over a Ni/Al2O3 catalyst in a coaxial dielectric barrier discharge reactor, J. Phys. D. Appl. Phys. 44 (2011) 274007. doi:10.1088/0022-3727/44/27/274007.

[25] H.L. Chen, H.M. Lee, S.H. Chen, M.B. Chang, S.J. Yu, S.N. Li, Removal of volatile organic compounds by single-stage and two-stage plasma catalysis systems: a review of the performance enhancement mechanisms, current status, and suitable applications., Environ. Sci. Technol. 43

(2009) 2216–27. http://www.ncbi.nlm.nih.gov/pubmed/19452866.

[26] A.M. Vandenbroucke, R. Morent, N. De Geyter, C. Leys, Non-thermal plasmas for non-catalytic and catalytic VOC abatement., J. Hazard. Mater. 195 (2011) 30–54. doi:10.1016/j.jhazmat.2011.08.060.

[27] J. Van Durme, J. Dewulf, C. Leys, H. Van Langenhove, Combining non-thermal plasma with heterogeneous catalysis in waste gas treatment: A review, Appl. Catal. B Environ. 78 (2008) 324–333. doi:10.1016/j.apcatb.2007.09.035.

[28] F. Thevenet, L. Sivachandiran, O. Guaitella, C. Barakat, a Rousseau, Plasma–catalyst coupling for volatile organic compound removal and indoor air treatment: a review, J. Phys. D. Appl. Phys. 47 (2014) 224011. doi:10.1088/0022-3727/47/22/224011.

[29] M.B. Kizling, S.G. Jaras, A review of the use of plasma techniques in catalyst preparation and catalytic reactions, Appl. Catal. A Gen. 147 (1996) 1–21.

[30] B.S. Patil, Q. Wang, V. Hessel, J. Lang, Plasma N2-fixation: 1900–2014, Catal. Today. 256 (2015) 49–66. doi:10.1016/j.cattod.2015.05.005.

[31] V. Hessel, G. Cravotto, P. Fitzpatrick, B.S. Patil, J. Lang, W. Bonrath, Industrial applications of plasma , microwave and ultrasound techniques : Nitrogen-fixation and hydrogenation reactions, Chem. Eng. Process. Process Intensif. 71 (2013) 19–30. doi:10.1016/j.cep.2013.02.002.

[32] S. Samukawa, M. Hori, S. Rauf, K. Tachibana, P. Bruggeman, G. Kroesen, et al., The 2012 Plasma Roadmap, J. Phys. D. Appl. Phys. 45 (2012) 253001. doi:10.1088/0022-3727/45/25/253001.

[33] C. Bramsiepe, S. Sievers, T. Seifert, G.D. Stefanidis, D.G. Vlachos, H. Schnitzer, et al., Low-cost small scale processing technologies for production applications in various environments — Mass produced factories, Chem. Eng. Process. Process Intensif. 51 (2012) 32–52. doi:10.1016/j.cep.2011.08.005.

[34] N. Krasberg, L. Hohmann, T. Bieringer, C. Bramsiepe, N. Kockmann, Selection of Technical Reactor Equipment for Modular, Continuous Small-Scale Plants, Processes. 2 (2014) 265–292. doi:10.3390/pr2010265.

[35] T. Seifert, S. Sievers, C. Bramsiepe, G. Schembecker, Small scale , modular and continuous : A new approach in plant design, Chem. Eng. Process. Process Intensif. 52 (2012) 140–150. doi:10.1016/j.cep.2011.10.007.

[36] B.S. Patil, Q. Wang, V. Hessel, J. Lang, Plasma Assisted Nitrogen Fixation Reactions, in: Altern. Energy Sources Green Chem., Royal Society of Chemistry, 2016.

[37] R. Ingels, D. Graves, S. Anderson, R. Koller, Modern Plasma Technology for Nitrogen Fixation:

New Opportunities?, in: Int. Fertil. Soc., International Fertiliser Society, London, UK, 2015: pp. 1–27. http://fertiliser-society.org/proceedings/uk/Prc771.HTM.

[38] W. Avery, A role for ammonia in the hydrogen economy, Int. J. Hydrogen Energy. 13 (1988) 761–773. doi:10.1016/0360-3199(88)90037-7.

[39] E. Morgan, J. Manwell, J. McGowan, Wind-powered ammonia fuel production for remote islands: A case study, Renew. Energy. 72 (2014) 51–61. doi:10.1016/j.renene.2014.06.034.

[40] D. Rapakoulias, S. Cavadias, J. Amouroux, Processus catalytiques dans un reacteur a plasma hors d'équilibre II. Fixation de l'azote dans le système N2-O2., Rev. Phys. Appl. 15 (1980) 1261–1265.

[41] B. Mutel, O. Dessaux, P. Goudmand, Energy Cost Improvement of The Nitrogen Oxides Synthesis in a Low Pressure Plasma, Rev. Phys. Appl. 19 (1984) 461–464.

[42] V.M. Belova, E.N. Eremin, A.N. Maltsev, Heterogeneous catalytic oxidation of nitrogen in a glow discharge II 1:1 nitrogen-oxygen mixture, Russ. J. Phys. Chem. 52 (1978) 968–970.

[43] E.N. Eremin, V.M. Belova, A.N. Maltsev, Heterogeneous catalytic oxidation of nitrogen inglow discharge III. N2:O2~1:4 Nitrogen-Oxygen mixture, Russ. J. Phys. Chem. 52 (1978) 970–972.

[44] Q. Sun, A. Zhu, X. Yang, J. Niu, Y. Xu, Formation of NOx from N2 and O2 in catalyst-pellet filled dielectric barrier discharges at atmospheric pressure., Chem. Commun. 5 (2003) 1418–9.

[45] T. Mizushima, K. Matsumoto, J. Sugoh, H. Ohkita, N. Kakuta, Tubular membrane-like catalyst for reactor with dielectric-barrier-discharge plasma and its performance in ammonia synthesis, Appl. Catal. A Gen. 265 (2004) 53–59. doi:10.1016/j.apcata.2004.01.002.

[46] B. Mingdong, B. Xiyao, Z. Zhitao, Synthesis of Ammonia in a Strong Electric Field Discharge at Ambient Pressure, Plasma Chem. Plasma Process. 20 (2000) 511–520.

[47] M. Bai, Z. Zhang, M. Bai, X. Bai, H. Gao, Synthesis of Ammonia Using CH4/N2 Plasmas Based on Micro-Gap Discharge under Environmentally Friendly Condition, Plasma Chem. Plasma Process. 28 (2008) 405–414. doi:10.1007/s11090-008-9132-4.

[48] L.R. O`Hare, Nitrogen fixation by plasma and catalyst, US 4451436, 1984.

[49] L.R. O`Hare, Nitrogen fixation by electric arc and catalyst, US 4877589, 1989.

[50] T.C. Manley, The Electric Characteristics of the Ozonator Discharge, Trans Electrochem. Soc. 84 (1943) 83–96. doi:10.1149/1.3071556.

[51] U. Kogelschatz, Dielectric-barrier Discharges : Their History, Discharge Physics, and Industrial Applications, Plasma Chem. Plasma Process. 23 (2003) 1–46.

[52] X. Tu, H.J. Gallon, J.C. Whitehead, Electrical and spectroscopic diagnostics of a single-stage

plasma-catalysis system: effect of packing with TiO 2, J. Phys. D. Appl. Phys. 44 (2011) 482003. doi:10.1088/0022-3727/44/48/482003.

[53] H.H. Kim, A. Ogata, Interaction of Nonthermal Plasma with Catalyst for the Air Pollution Control, Int. J. Plasma Environ. Sci. Technol. 6 (2012) 43–48.

[54] D. Mei, X. Zhu, Y.-L. He, J.D. Yan, X. Tu, Plasma-assisted conversion of CO2 in a dielectric barrier discharge reactor: understanding the effect of packing materials, Plasma Sources Sci. Technol. 24 (2015) 015011. doi:10.1088/0963-0252/24/1/015011.

[55] G. Arlt, D. Hennings, G. De With, Dielectric properties of fine-grained barium titanate ceramics, J. Appl. Phys. 58 (1985) 1619–1625. doi:10.1063/1.336051.

[56] H.L. Chen, H.M. Lee, S.H. Chen, M.B. Chang, Review of Packed-Bed Plasma Reactor for Ozone Generation and Air Pollution Control, Ind. Eng. Chem. Res. 47 (2008) 2130.

[57] B.S. Patil, J. Rovira Palau, V. Hessel, J. Lang, Q. Wang, Plamsa Nitrogen Oxides Synthesis in a Milli-Scale Gliding Arc Reactor: Investigating the Electrical and Process Prameters, Plasma Chemsiry Plasma Process. 36 (2016) 241–257. doi:10.1007/s11090-015-9671-4.

[58] V.D. Sokolovskii, Principles of Oxidative Catalysis on Solid Oxides, Catal. Rev. 32 (1990) 1–49. doi:10.1080/01614949009349939.

[59] J.P.A. Neeft, M. Makkee, J.A. Moulijn, Catalysts for the oxidation of soot from diesel exhaust gases. I. An exploratory study, Appl. Catal. B Environ. 8 (1996) 57–78. doi:10.1016/0926-3373(95)00057-7.

[60] A. Gicquel, S. Cavaidas, J. Amouroux, Heterogeneous catalysis in low-pressure plasmas, J. Phys. D. Appl. Phys. 19 (1986) 2013–2042.

[61] V.D. Rusanov, a a Fridman, G. V Sholin, The physics of a chemically active plasma with nonequilibrium vibrational excitation of molecules, Sov. Phys. Uspekhi. 24 (1981) 447–474. doi:10.1070/PU1981v024n06ABEH004884.

[62] V.D. Rusanov, A.A. Fridman, G. V Sholin, Physics of chemically active plasma with inequilibrium vibrational excitation of molecules, Usp. Phys. Nauk. 134 (1981) 185–231.

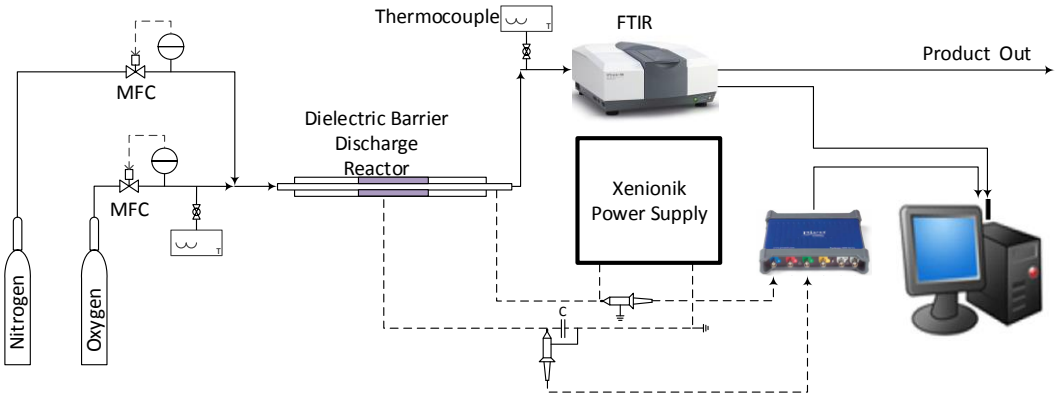

Fig. 1. A Scheme of the one-sided DBD plasma experimental set-up.

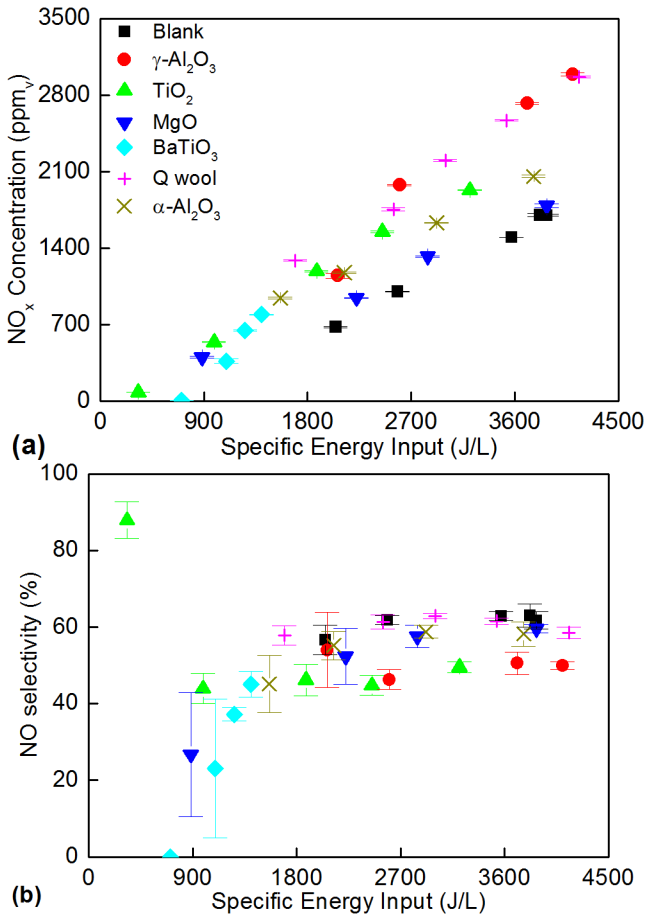

Fig. 2. (a) The effect of catalyst support on NO_x concentration. (b) The effect of specific energy input on the NO selectivity.

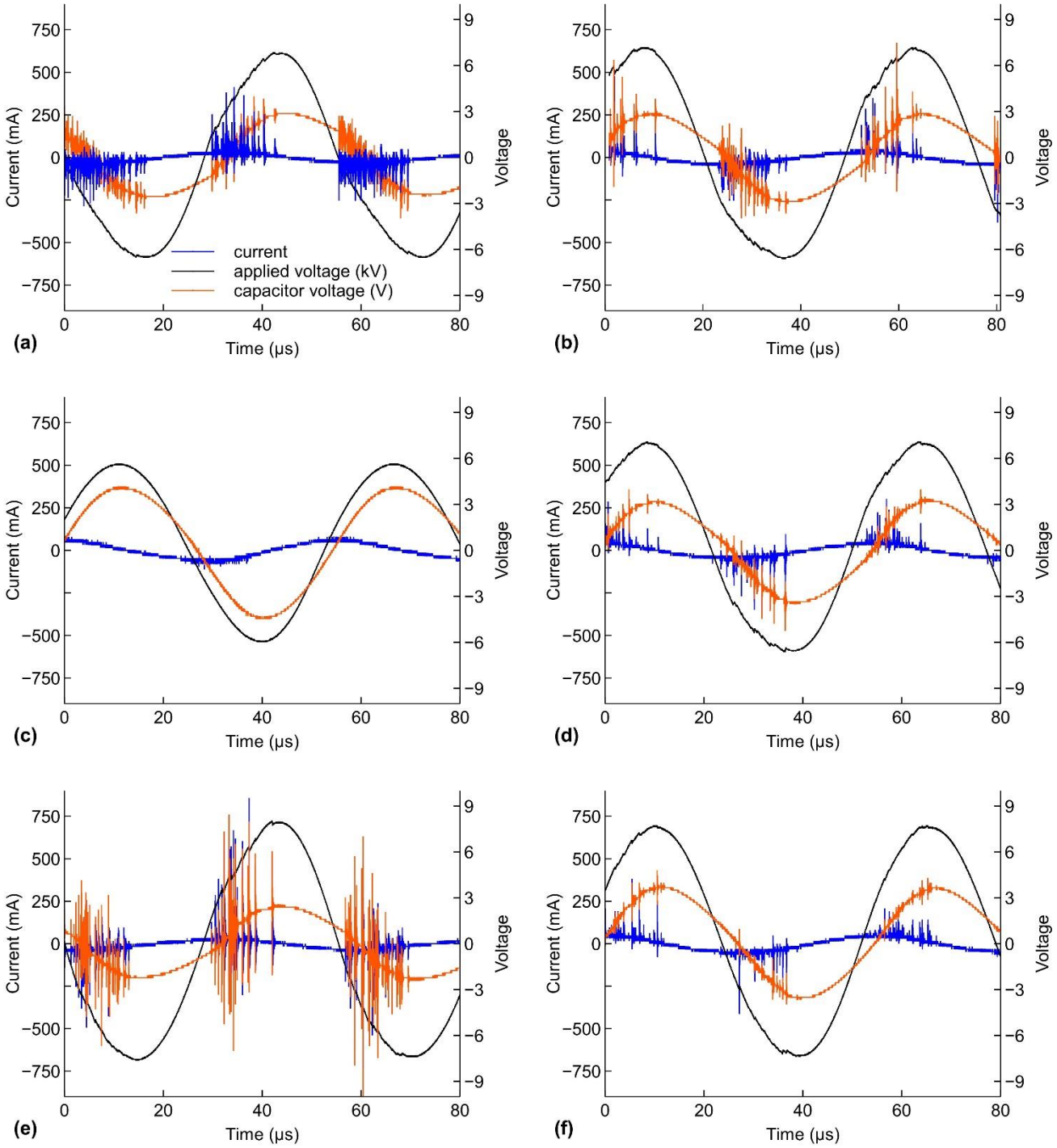

Fig. 3. Discharge signals for various packing materials at a plasma power of 45 watts; (a) the blank experiment without packing, (b) γ-Al_2O_3, (c) $BaTiO_3$, (d) MgO, (e) Quartz wool, (f) TiO_2 (at 18 kHz, 20 μs, flow rate of 1

L/min, N_2/O_2 ratio of 1).

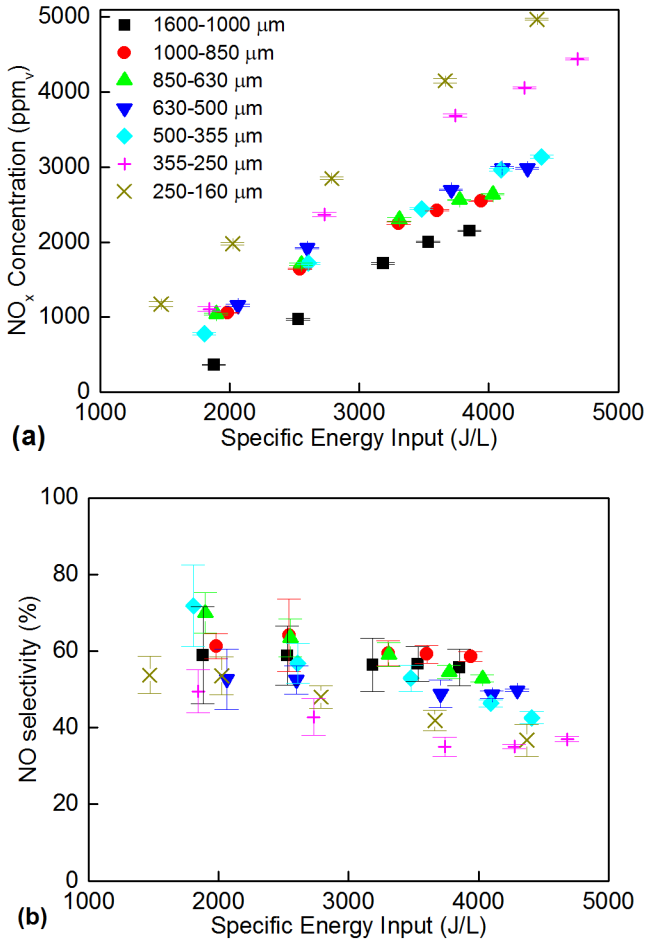

Fig. 4. The effect of the catalyst support (γ-Al_2O_3) particle size (a) on NO_x concentration and (b) the selectivity towards NO. (Flow rate of 1 L/min and N_2/O_2=1 at frequency of 18 kHz and pulse width of 20 μs.)

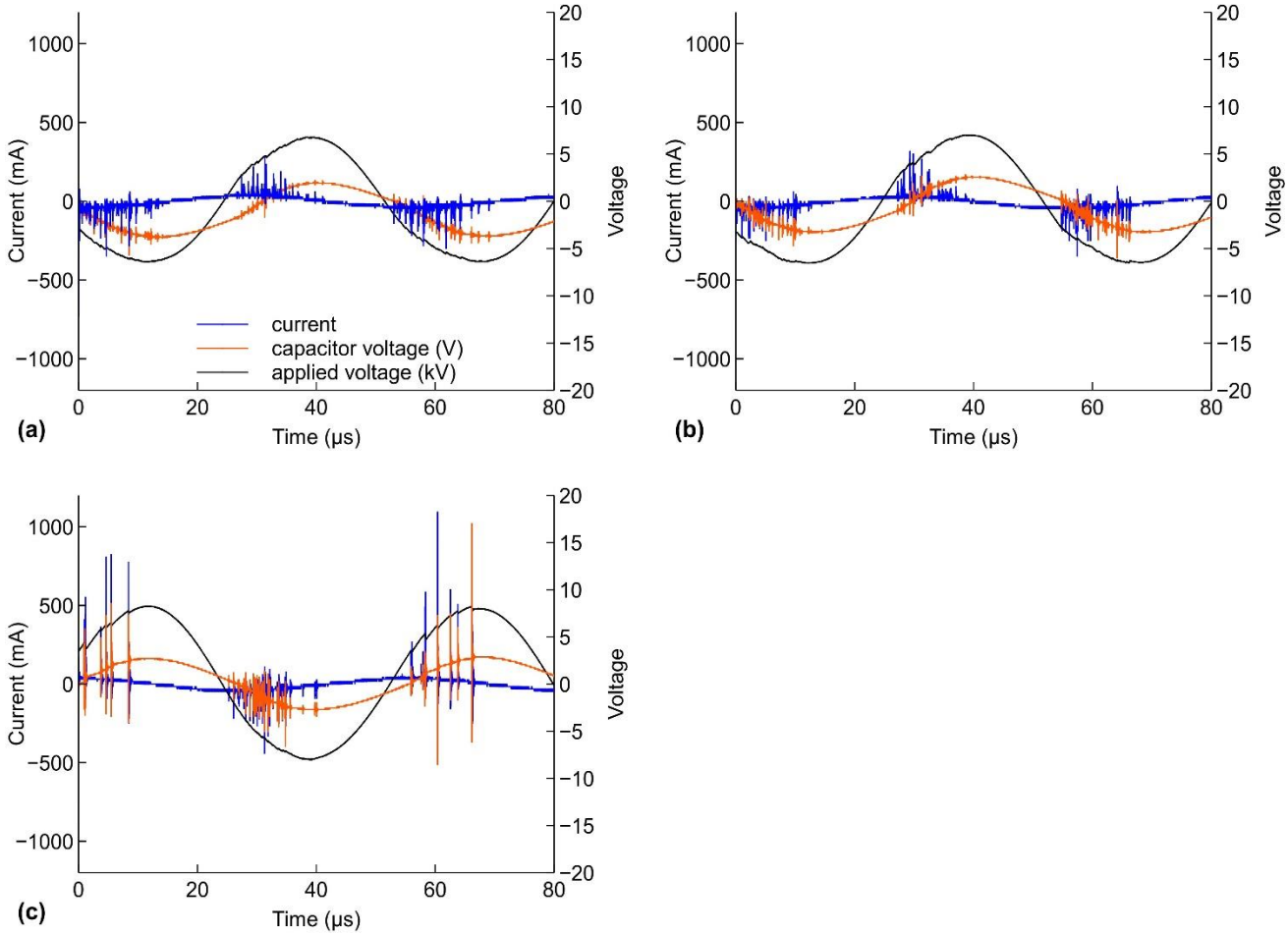

Fig. 5. Discharge signals at a plasma power of 45 watts, 18 kHz, 20 μs, flow rate of1 L/min and N_2/O_2 ratio of 1 for the DBD reactor packed with γ-Al_2O_3 with the particle diameters of (a) 1600-1000 μm, (b) 850-630 μm, (c) 350-250 μm. The following designations are used: (blue) current, (black) applied voltage, (blue) capacitor voltage.

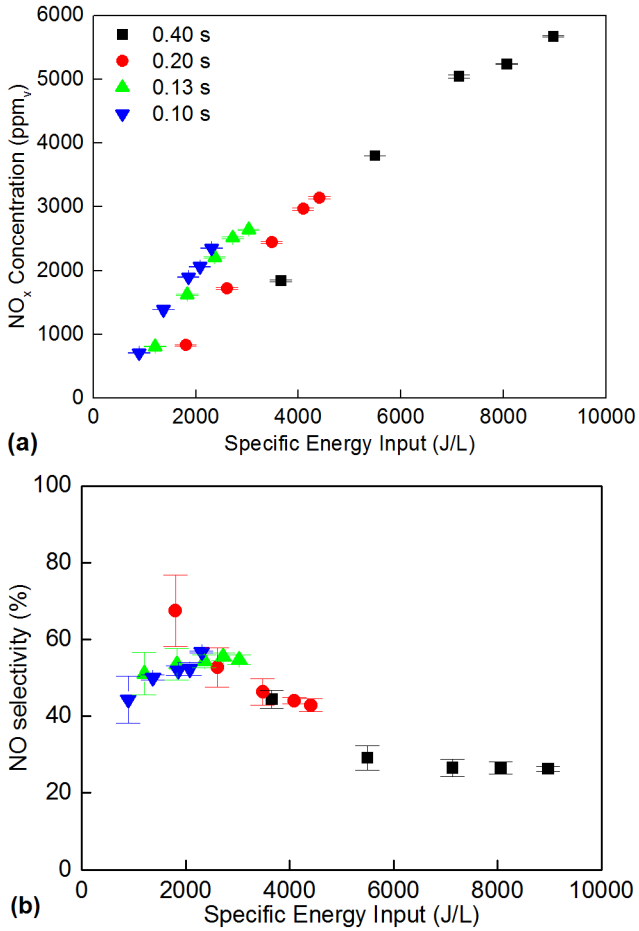

Fig. 6. The effect of the residence time for γ-Al_2O_3 packed DBD reactor on (a) NO_x concentration and (b) the selectivity towards NO. (Particle size= 500-355 micron, 18 kHz, 20 μs).

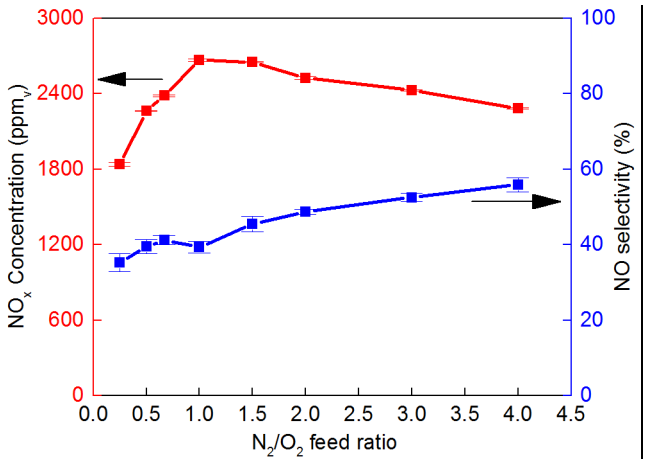

Fig. 7. The effect of feed ratio on NO_x concentration and NO selectivity in a DBD packed with γ-Al_2O_3 particles 500-355 μm at the total gas flow rate of 1 L/min.

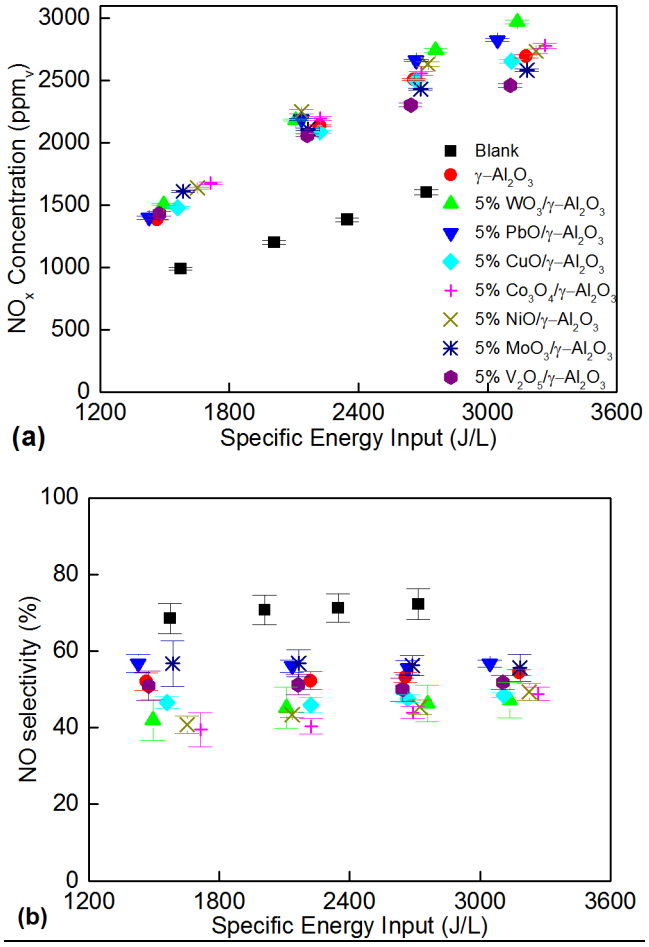

Fig. 8. The effect of metal oxides supported over γ-Al_2O_3 on (a) NO_x concentration and (b) the selectivity towards NO.

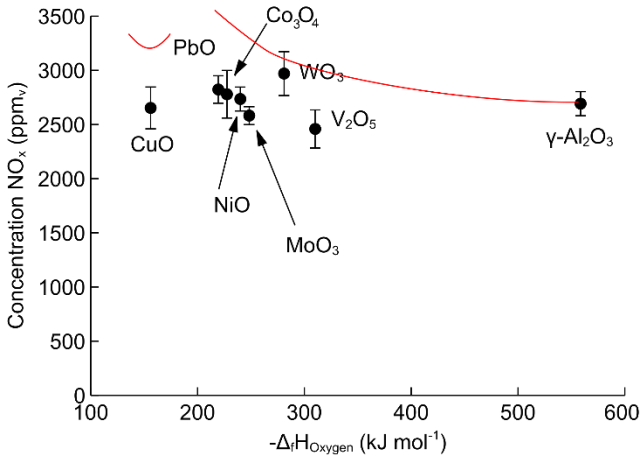

Fig. 9. NO_x concentration for the studied 5% alumina-supported catalysts at the highest specific energy input as a function of oxygen "binding" energy (standard enthalpy of oxide formation per oxygen atom) with the (red) general trend on the expected concentration in case of a limiting step of oxygen activation.

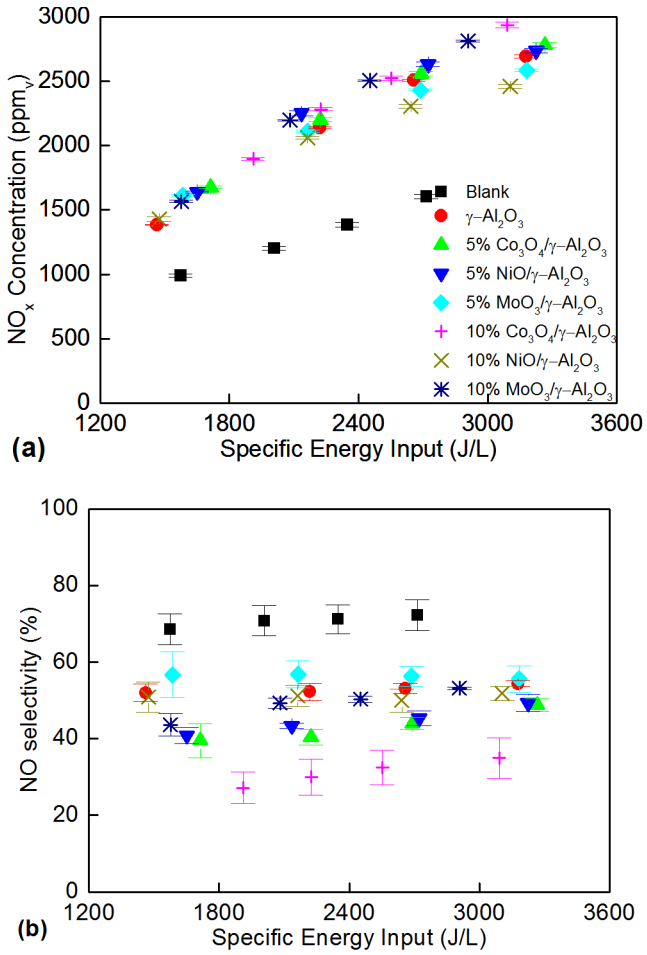

Fig. 10. The effect of the supported oxide loading on (a) on NO_x concentration and (b) the selectivity towards NO.

Table 1. Properties of support materials.

Support Type	**Surface Area(m^2g^{-1})**	**Relative dielectric constant**
γ-Al_2O_3	112	9.3-11.5
α-Al_2O_3	0.3	9.3
TiO_2	34	85
MgO	0.03	9.7
$BaTiO_3$	0.1	400-6500
Quartz Wool	0.5	4.6